3D seismic-well correlation workflow in depth domain using an evolutionary algorithm and machine learning interpolation

Matheus Freire Souza Barcelos Guimarães (GIR/LENEP/UENF),
Fernando Sergio Moraes (GIR/LENEP/UENF, INCT-GP/CNPq),
Carlos André Martins Assis de Assis (CGG),
Sérgio Adriano Moura Oliveira (GIR/LENEP/UENF, INCT-GP/CNPq)

Abstract

Seismic interpretation is a process to identify the hydrocarbon occurrence in deep water reservoirs. Correlating the structural and stratigraphic interpretation with well markers in the depth domain is complex. This research presents a workflow designed to perform precise seismic-well tie in the depth domain. The proposed workflow uses evolutionary and machine learning algorithms in order to adjust a velocity field. This process can be applied even without the previous velocity field obtained from velocity analysis. The proposed workflow allows not only a precise seismic data positioning in the depth domain but also the estimation of the velocity and impedance.

Introduction

A consistent representation of seismic data in depth helps to reduce risks in exploration projects. The problem is that the seismic-to-well tie procedure is conventionally done in the time domain by a stretch-squeeze process applied to the well logs, and depth conversion does not preserve well ties. As a result, most of the interpretation work is restricted to the two way travel time domain.

According to Etris et al. (2001), seismic interpretation in the time domain for stratigraphic analysis is acceptable since the interpretation remains the same despite structural changes. Otherwise, the structural interpretation in the time domain is not recommended due to the ambiguity of the real position and format of the geological structures. This ambiguity occurs due to the assumption of constant velocities for the layers. To solve this ambiguity and perform an accurate structural interpretation, applying a depth conversion process using a proper conversion equation and a high-resolution velocity field is necessary. Several equations available for Time-Depth conversion can be applied according to the available velocity data and the image ray concept (Filpo et al., 2016) is relevant due to the good results even in areas with high-complexity geology formations.

The primary process to build a high-resolution velocity field is the Full Waveform Inversion (FWI). This process extracts the velocity information from the full content of the seismic trace (Virieux et al., 2014). However, despite the good results, this process requires pre-stack seismic data that can not be available (as in the case of this present research). In those cases, the velocity information can be obtained by building a low-frequency model interpolating the velocity from well log data (Sams and Carter, 2017; Kumar and Negi, 2012).

Sometimes, the position of interpreted seismic horizons do not correlates with the well markers, what happens due to geological complexity (Mancini, 2013; Viloria et al., 2009; Gupta et al., 2013). Therefore, we developed a workflow that minimizes the difference between the seismic horizon and the well markers in the depth domain by updating the velocity field generated by interpolating the well logs along the interpreted horizons. The proposed workflow estimates precise seismic data in the depth domain without the previous information about the velocity data from the velocity analysis. The low-frequency velocity model obtained in this process can be used to estimate the absolute acoustic impedance.

Method

The present research was applied in the northwest area of Tupi field in Santos Basin in Brazilian pre-salt Figure 1. The area represented in Figure 1 has 19 km^2 and the available data is composed of a post-stack 3D seismic volume and eight wells with the main log curves (gamma-ray, resistivity, sonic, and density) and the Vertical Seismic Profile (VSP) data. The general workflow is represented in Figure 2, where we present the full process to obtain the seismic data in the depth domain.

The workflow starts with the estimation of the relative acoustic impedance by applying the Colored Inversion (Lancaster and Whitcombe, 2000) and adapted by Blouin and Gloaguen (2017). The colored inversion is a robust process that enhances the seismic data, enabling a more robust interpretation of the geological structures. The colored inversion is fast, so it was choose to generate impedance to be used as an input attribute to train the machine learning algorithm and seismic horizon interpretation.

To build the low-frequency velocity field, we use the well log information. Unfortunately, this log was registered only in the reservoir depth interval (4800 to 5500 meters). Thus, we apply a machine learning algorithm, Extremely Randomized Trees (ExtraTrees), to estimate the velocities to fill the well range. The ExtraTrees is a tree-based ensemble method developed by Geurts et al. (2006). This algorithm consists of a strongly randomized process to build

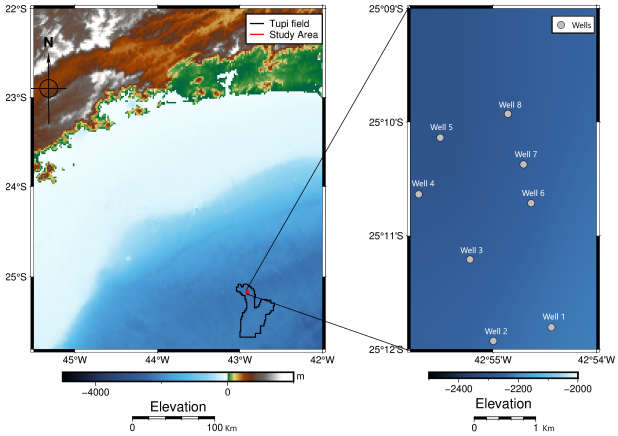

Figure 1: Study area location and wells distribution.

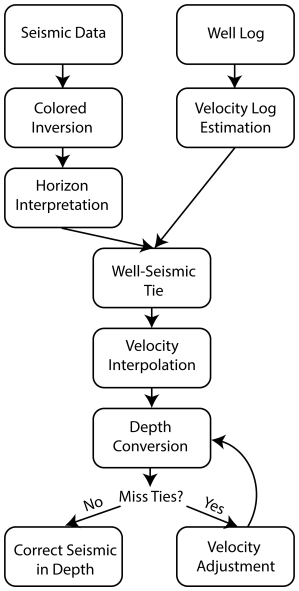

Figure 2: General description of the proposed workflow.

the decision tree, where the structures are independent of the output value of the learning sample. The randomized process constructs a more robust algorithm reducing the influence of noise, bias, and variance (Saeed et al., 2021).

Reference velocity information is required to estimate the velocity log for the full range of the well using the Extra-Trees. The VSP data gives information on the interval velocity along the well. Since this data represent a constant velocity between the layers in depth, we use other curves (gamma-ray and resistivity) that are fully registered along the well, and the seismic attributes impedance and cosine phase, extracted on the positions of the wells, to estimate the interval velocity with a log shape.

The next step of the workflow consists of the horizon interpretation. In this step, we map the structural variation of the main formations of the study area. The structures mapped were the ground level, the top and base of the salt dome, the Barra Velha formation, and the basement. This process was performed using the OpenDtect software. We construct the horizon cube from those five horizons by applying the method described by de Groot et al. (2010). The horizon cube is an auto-tracker to identify multiple structures between the initial horizons using the seismic dip field. The high density of horizons generated is used to interpolate the velocity following geology structural variation.

The interpolation process along the horizons requires the well log data in the time domain. This correlation is usually done with the well-seismic-tie with a stretch-squeeze process that results in some distortions of the well log information. To avoid that, we apply the well-seismic tie methodology developed by Gelpi et al. (2020). The proposed method ties the well by applying a distortion process on the velocity log and a rotation of the wavelet phase. The authors use the differential evolution algorithm to estimate the distortion for the velocity and the phase of the wavelet, which minimizes the difference between the synthetic seismogram and the seismic trace. The differential evolution algorithm is a global optimization method that relies on mutation, recombination, and selection to evolve a collection of candidate solutions toward an optimal state (Price, 2013).

We can build the low-frequency velocity field by correlating the well log with the seismic data in the time domain. Figure 3 shows the process. The interpolation starts extracting the velocities values of the horizon and well log time intersection. This process gives the individual velocity values for each horizon generated in the horizon cube and retains the velocity variation inside the layers. The interpolation process uses the ExtraTrees algorithm. To train the algorithm, we use the positional information (Inline, Crossline, and time) and the seismic attributes (impedance and cosine phase). After the interpolation process, the velocities horizons are concatenated and resampled to the time interval of seismic data (4 ms). For the water layer velocity, we use 1500 m/s. For deeper sections below the basement position, we use the highest velocities of the last horizon to compose the low-frequency velocity field.

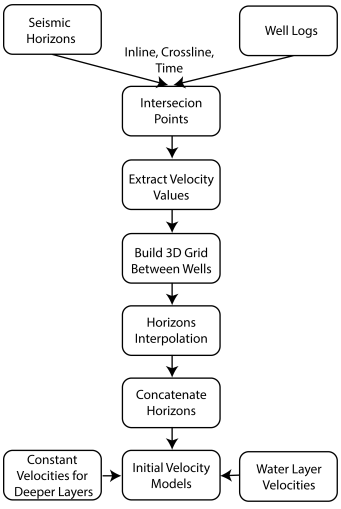

Figure 3: Workflow to build the low-frequency velocity field.

To analyze the reliability of the velocity field, we perform

a time-to-depth conversion using the OpenDtect software. The software applies the Dix (1955) for this process

$$z = \frac{1}{2}\int_0^t v_d(t)dt \quad (1)$$

where z is the depth, t is the time, and v_d is the velocity. Using this linear equation for depth conversion, as expected for a complex geological area as the pre-salt, the horizons depth position is not correlated to the well markers. Figure 4 shows the process of adjusting the velocity data to minimize the difference between the horizons and well markers position in depth. To perform this adjustment, we apply a distortion factor for the velocity extracted on the positions of the wells (Inline and Crossline). This distortion factor is estimated using the differential evolution algorithm, which minimizes the difference between the horizon depth in 1 and the corresponding well marker depth value. The process progressively adjusts the shallow layer (ground level) to the deepest layer (Barra Velha formation).

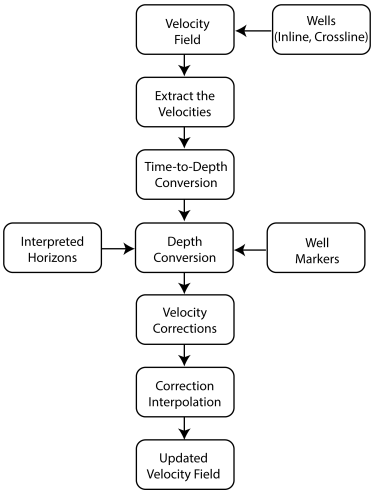

Figure 4: Workflow to adjust the velocities for seismic-well tie in the depth domain.

Results

The application of the proposed workflow has three steps: the well log estimation process, the interpolation along the horizons, and the velocity correction for time-to-depth conversion.

Filling the velocity log for the well range requires two steps: filling the salt section for some wells using other wells as reference and filling the post-salt area for all the wells using the VSP interval velocity as a reference. The initial condition of the velocity logs is shown in Figure 5. Wells 1, 2, 3, 6, and 8 have the velocity log curve registered from the top of the salt to the reservoir (3000 to 5500 meters). We train the ExtraTrees to estimate these logs velocities using the log curves (gamma-ray and resistivity) and the seismic attributes (impedance and cosine phase) as attributes. Then, we predict the velocities for wells 4, 5, and 7 to fill the salt section. The post-salt section velocity estimation was performed similarly, using the same attributes to estimate the interval velocity of VSP. The best results, where the estimated velocity curves had a log shape, were obtained for wells 1 and 4. We use this result to estimate the post-salt velocity for all the other wells. The application of ExtraTrees using other logs curves to train the model allows the predicted velocity follows the log frequency on the range of interval velocity. The result of velocity estimation process is shown in Figure 5. We use a moving average filter to smooth the logs for the interpolation process.

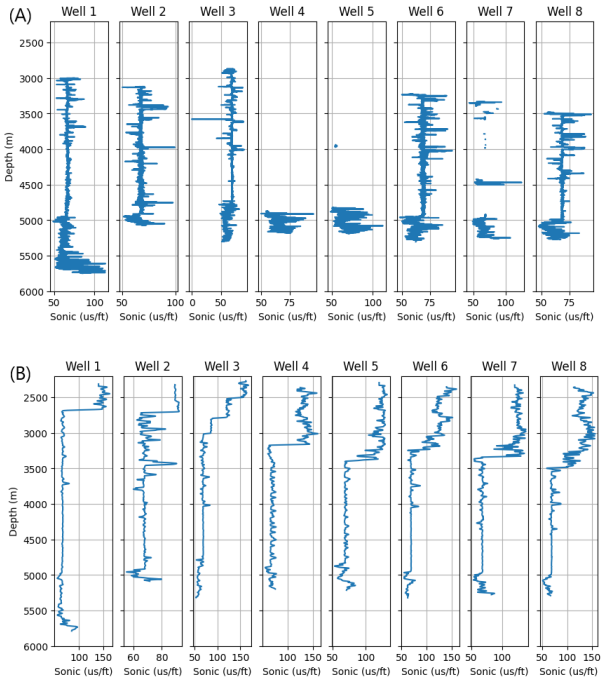

Figure 5: Imputation process for velocity logs. (A) Initial condition of the logs; (B) Result of the velocity estimation process.

Figure 6 (A and B) shows the initial grid between the wells and Figure 6 (C and D) the result of interpolation along the horizons. The velocity values obtained along the horizons follows the variation on the initial grid. The good correlation shows the efficiency of the ExtraTrees to estimate the velocity values. Figure 7 shows initial low-frequency velocity field. The interpolation process shows a good fit for the expected velocity variation for each layer. The individual interpolation along each horizon of the horizon cube allows the velocity field follows the structural variation of the study area and keep the velocity variation inside the layers. This is an important information since some studies have been developed to identify the velocity variation in salt stratification (Falcão et al., 2016; Gobatto et al., 2016).

The depth conversion process using the initial velocity model (figure 8 A) shows a difference between the horizons and well markers of the top and base of salt at around 100 meters (figure 8 B). This difference can be related to applying the Dix conversion equation for a complex geology area as the pre-salt. Figure 8 C shows the corrected velocity field and figure 8 D shows the depth conversion result using the updated velocities. Table 1 shows the distortion factor applied. We must apply two iterations to obtain the seismic data in the depth domain correlated to the well markers.

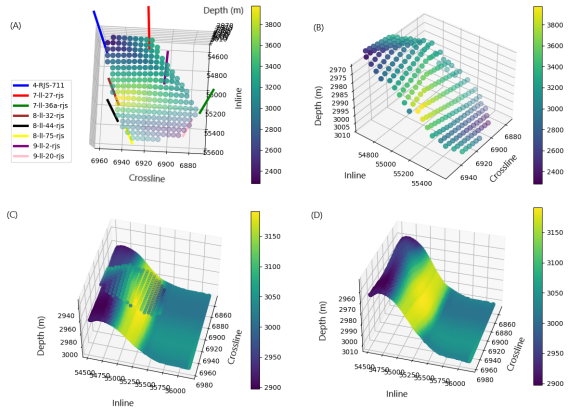

Figure 6: Result of interpolation process. (A - B) Initial velocity grid between the wells; (C) Comparison of grid size (400 points) and the horizon (41000 points); (D) Velocity Horizon example.

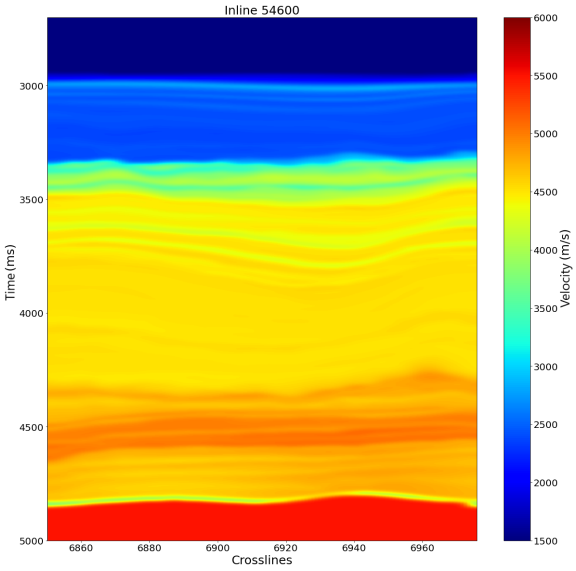

Figure 7: Initial low-frequency velocity field.

It was necessary because the attributes used to train the model (inline, crossline, time, and velocity) do not have a high correlation to the distortion factor. In this case, we can observe the variation of distortion factor in Table 1 reduces each iteration until the correct position of the seismic horizons.

The proposed methodology for low-frequency model building enables the estimation of the absolute acoustic impedance. This process requires the combination of the low-frequency component and the relative acoustic impedance, applying the following equation

$$IP_{abs} = IP_{lf} + \alpha * IP_{rel} \quad (2)$$

where the IP_{abs} is the absolute acoustic impedance, IP_{lf} is the low-frequency acoustic impedance, IP_{rel} is the relative acoustic impedance, and α is a scale factor estimated by

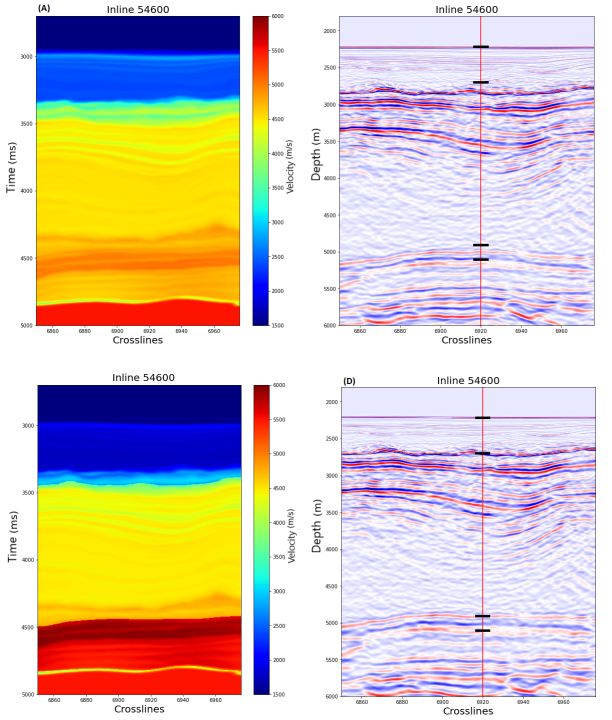

Figure 8: Result of velocity field adjustment and time-to-depth conversion. (A) Initial velocity field; (B) Depth conversion with miss ties between horizons and well markers; (C) Corrected velocity field; (D) Seismic-well tie in deepth domain.

$$\alpha = \frac{RMS(IP_{well})}{RMS(IP_{rel})} \quad (3)$$

where RMS is the root-mean-square and IP_{well} is the acoustic impedance log filtered with a band-pass on the same frequency of the seismic data (5-40 Hz). Figure 9 shows the result of the absolute acoustic impedance in the depth domain and the correlation to the well log. We can observe a high correlation between the log variation and the absolute acoustic impedance field stratification. This result is an important tool for seismic interpretation due to the accuracy of depth positioning and the relevant information on acoustic impedance to identify hydrocarbon occurrence in the study area.

Conclusions

Applying the proposed workflow for the study area enables a precise correlation of the seismic data in the depth domain to the well markers, even without the previous velocity information from velocity analysis. The low-frequency velocity field obtained in this study reliably represents the geology of the study area. Using a machine learning algorithm to interpolate the well log velocity enables more reliable velocity estimation for all the seismic volume. Therefore, using highly correlated attributes is important to precisely estimate the seismic volume's velocity. Applying the interpolation for each horizon individually enables the velocity to follows the structural variation. Using an evolu-

Table 1: Distortion factor applied to correct the velocity for time-to-depth conversion. The process needs two iterations to minimize the difference between the seismic horizon and the well log markers.

Corrections	Horizons	Well 1	Well 2	Well 3	Well 4	Well 5	Well 6	Well 7	Well 8
Iteration 1	Ground Level	1,010538	0,9978	0,9972	1,00275	1,00005	1,03558	1,0219	1,0271
	Top of Salt	0,7	0,7381	1,1999	0,76758	0,83955	0,88007	0,8671	0,9148
	Base of Salt	0,9983635	0,9887	0,8822	1,05714	1,13118	0,9467	0,9333	0,8692
	Barra Velha	0,9319422	1,1834	1,1265	1,3	1,09047	0,7	1,0078	1,2127
Iteration 2	Ground Level	1,0004237	1,0004	0,9997	1,00045	0,99996	0,99993	1,0002	1,0001
	Top of Salt	1,0064645	1,0021	0,9993	1,00064	1,00033	1,00023	1,0003	1,0002
	Base of Salt	0,9994157	1	0,995	1,00104	1,00108	1,00208	1,0001	0,9957
	Barra Velha	0,9929234	1,0086	1,0123	1,06135	1,00484	0,92026	1,0059	1,0133

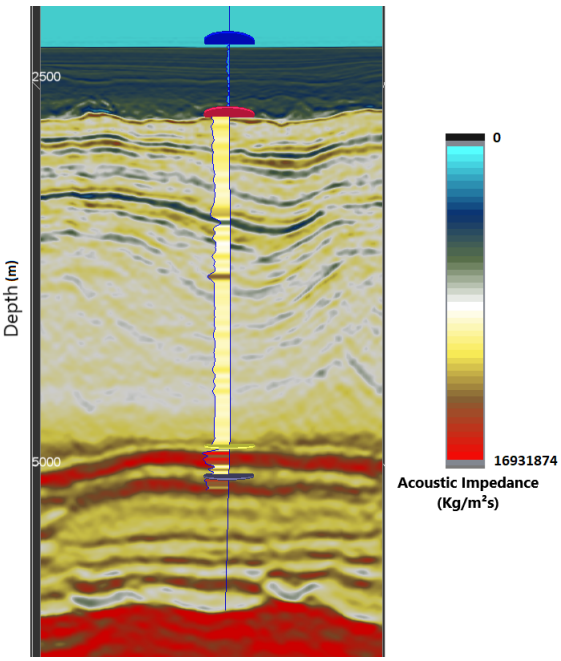

Figure 9: Resulted Acoustic Impedance field and comparison with the acoustic impedance log.

tionary algorithm facilitates the estimation of velocity adjustment to minimize the difference between the seismic data in depth and well markers. Applying the derived low-frequency model to estimate the absolute acoustic impedance enables the development of more detailed studies for reservoir characterization in the depth domain. Finally, the proposed workflow estimates important parameters (velocity and acoustic impedance) in depth positioning that ties to the well markers.

Acknowledgments

We thank the ANP for the available dataset, the Dgb Earth Science for the OpenDtect software license, and the Geoactive for the Interactive Petrophysics software license. We also want to thank the professors and colleagues who help with the discussions and suggestions for the research development.

References

Blouin, M., and E. Gloaguen, 2017, Colored inversion: The Leading Edge, **36**, 858–861.

de Groot, P., A. Huck, G. de Bruin, N. Hemstra, and J. Bedford, 2010, The horizon cube: A step change in seismic interpretation!: The Leading Edge, **29**, 1048–1055.

Dix, C. H., 1955, SEISMIC VELOCITIES FROM SURFACE MEASUREMENTS: GEOPHYSICS, **20**, 68–86.

Etris, E. L., N. J. Crabtree, and J. Dewar, 2001, True depth conversion: more than a pretty picture.

Falcão, L., A. Maul, F. Gobatto, G. González, and M. D. L. Á. González, 2016, RESULTS OF INCORPORATING THE STRATIGRAPHY WITHIN THE EVAPORITIC SEQUENCE INTO THE VELOCITY FIELD FOR RESERVOIR CHARACTERIZATION: Revista Brasileira de Geofísica, **34**.

Filpo, E., R. Portugal, N. Zago, P. M. Cunha, A. Vicentini, and J. L. Carbonesi, 2016, Image-ray concept as the key to 20 years of success of time-to-depth conversion in petrobras: The Leading Edge, **35**, 323–328.

Gelpi, G. R., D. O. Pérez, and D. R. Velis, 2020, Automatic well tying and wavelet phase estimation with no waveform stretching or squeezing: GEOPHYSICS, **85**, D83–D91.

Geurts, P., D. Ernst, and L. Wehenkel, 2006, Extremely randomized trees: Machine Learning, **63**, 3–42.

Gobatto, F., A. Maul, L. Teixeira, G. González, L. Falcão, M. González, and J. T. Boechat, 2016, Refining velocity model within the salt section in santos basin: An innovative workflow to include the existing stratification and its considerations: Presented at the SEG Technical Program Expanded Abstracts 2016, Society of Exploration Geophysicists.

Gupta, A., T. Muralimohan, C. Varadarajan, S. Singh, and P. Kumar, 2013, Well tie tomography an accurate time-depth conversion: Presented at the .

Kumar, N., and S. S. Negi, 2012, Low frequency modeling and its impact on seismic inversion data: Presented at the .

Lancaster, S., and D. Whitcombe, 2000, Fast-track 'coloured' inversion: Presented at the SEG Technical Program Expanded Abstracts 2000, Society of Exploration Geophysicists.

Mancini, F., 2013, A simplified workflow for accurate time-to-depth conversion using 3d grid tomography: The Leading Edge, **32**, 430–434.

Price, K. V., 2013, Differential evolution, *in* Handbook of Optimization: Springer Berlin Heidelberg, 187–214.

Saeed, U., S. U. Jan, Y.-D. Lee, and I. Koo, 2021, Fault diagnosis based on extremely randomized trees in wireless sensor networks: Reliability Engineering &amp System Safety, **205**, 107284.

Sams, M., and D. Carter, 2017, Stuck between a rock and a reflection: A tutorial on low-frequency models for seismic inversion: Interpretation, **5**, B17–B27.

Viloria, R., I. Garcia, A. Caudron, R. Cariel, F. D. Caires, J. G. Hernandez, and A. Bustos, 2009, Using a fine-tuned interval velocity model for improving the quality of time-to-depth conversion: The Leading Edge, **28**, 1430–1434.

Virieux, J., A. Asnaashari, R. Brossier, L. Métivier, A. Ribodetti, and W. Zhou, 2014, 6. an introduction to full waveform inversion, *in* Encyclopedia of Exploration Geophysics: Society of Exploration Geophysicists, R1–1–R1–40.